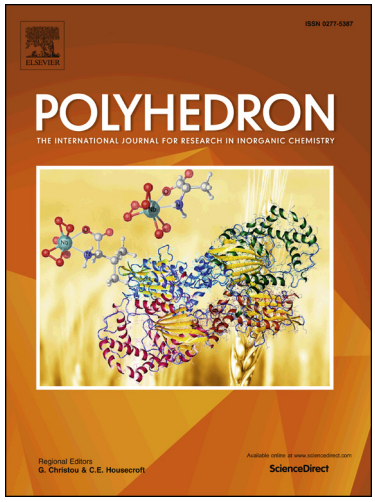

Synthesis, DNA binding and antibacterial activity of metal(II) complexes of a benzimidazole Schiff base

Khalid Mahmood, Waleed Hashmi, Hammad Ismail, Bushra Mirza, Brendan Twamley, Zareen Akhter, Isabel Rozas, Robert J. Baker

PII: S0277-5387(18)30656-9
DOI: https://doi.org/10.1016/j.poly.2018.10.020
Reference: POLY 13494

To appear in: *Polyhedron*

Received Date: 31 August 2018
Revised Date: 3 October 2018
Accepted Date: 5 October 2018

Please cite this article as: K. Mahmood, W. Hashmi, H. Ismail, B. Mirza, B. Twamley, Z. Akhter, I. Rozas, R.J. Baker, Synthesis, DNA binding and antibacterial activity of metal(II) complexes of a benzimidazole Schiff base, *Polyhedron* (2018), doi: https://doi.org/10.1016/j.poly.2018.10.020

Synthesis, DNA binding and antibacterial activity of metal(II) complexes of a benzimidazole Schiff base

Khalid Mahmood,[a] Waleed Hashmi,[b] Hammad Ismail,[c] Bushra Mirza,[b] Brendan Twamley,[d] Zareen Akhter,*[a] Isabel Rozas,*[d] and Robert J. Baker*[d]

[a] Department of Chemistry, Quaid-i-Azam University of Islamabad, Pakistan
[b] Department of Biochemistry, Quaid-i-Azam University of Islamabad, Pakistan
[c] Department of Biochemistry and Biotechnology, University of Gujrat, Pakistan
[d] School of Chemistry, Trinity College Dublin, The University of Dublin, Dublin 2, Ireland

*Corresponding authors:
Zareen Akhter, E-mail: zareen_a@qau.edu.pk
Isabel Rozas, E-mail: rozasi@tcd.ie
Robert J. Baker, E-mail: bakerrj@tcd.ie

Abstract

The benzimidazole derivative (*E*)-2-((4-(1*H*-benzo[*d*]imidazol-2-yl)phenylimino)methyl)-4-bromo phenol and the corresponding Zn(II), Ni(II), Cu(II), and Pd(II) complexes were prepared. The synthesized ligand and complexes were fully characterized and the ligand structure confirmed by single crystal X-ray diffraction analysis. The ability of this compound and its complexes to bind to DNA was first investigated with DNA thermal denaturation experiments, in general showing weak interactions. Additionally, UV-vis absorption spectroscopy was used to assess the binding to DNA and the corresponding binding constants (K_b) were calculated suggesting an intercalative mode of binding for the benzimidazole ligand. All compounds were screened for their antibacterial activity and the Ni(II) complex showed promising results against all bacterial strains (Gram positive and Gram negative) while the rest of the compounds showed activity against selective strains.

Graphical Abstract

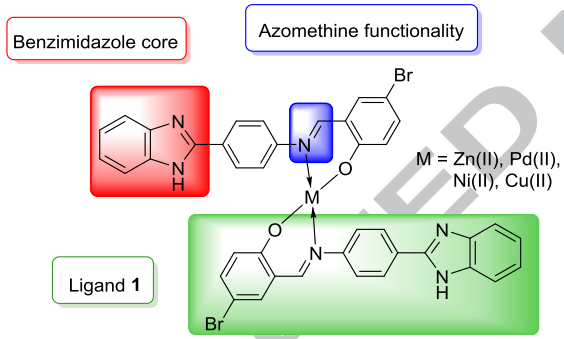

Synopsis

Several metal complexes of a benzimidazole Schiff base were prepared and characterised showing moderate DNA binding as intercalators and interesting activity against Gram positive and negative bacteria.

Keywords: benzimidazole • Schiff base • metallodrug • DNA-interaction • antibacterial

1. Introduction

Considering the lack of new antibiotics in the market, there is a high risk of an uncontrolled spread of resistant pathogens. The increase in the incidence of chronic infections represents an added problem because many of these diseases are untreatable due to resistance. There are many possible targets in bacteria, and one that has recently attracted much attention is DNA [1].

Thus, many DNA binding drugs have shown antimicrobial activity [2]. For example, the DNA intercalator echinomycin is more effective against clinical isolates of methicillin-resistant *Staphylococcus aureus* (MRSA) than the clinically used vancomycin not only in vitro but also in vivo in mice [3]. Additionally, derivatives of the DNA binder metallo-complex $[CoL_3]^{2+}$ containing 2,2-bipyridine, 1,10-phenanthroline, imidazole, methylimidazole, ethylimidazole or dimethylimidazole, have been reported to show antibacterial activity against *Escherichia coli*, *Salmonella typhimurium*, *S. aureus* or *Enterococcus faecalis*, among others [4,5].

With the aim of avoiding antibacterial resistance, the FDA has approved broad-spectrum antibiotics such as the Cu complexes of lomefloxacin [6] or ciprofloxacin [7], which act by inhibiting DNA gyrase activity and have demonstrated activity against both Gram positive and Gram negative bacteria, with MIC values around 0.3–2.6 μM. Another important DNA-binding agent is the minor groove binder pentamidine, which has been clinically used since the 1940s against a number of protozoal diseases. It was found that metals can really enhance the antibacterial activity of groove binders and, thus, while pentamidine analogue bis-(3-(4-dimethylaminophenyl)allylidene)-1,2-diaminoethane shows MIC values of 250 and 125 μg mL^{-1} for *B. subtilis* and *E. coli*, respectively, its Zn(II) complex has MIC values around 0.49 μg mL^{-1} for both bacteria [8].

Regarding suitable ligands for this type of potential metallodrugs, the benzimidazole heterocycle (Figure 1), which is found in commercial drugs such as omeprazole, mebendazole, and astemizole [9], is present in many biologically important DNA minor groove binding molecules such as Hoechst-33258 and Hoechst-33342 [10], as well as in several antimicrobials [11]. This type of derivative is also reported as mitochondria targeting photocytotoxic agent [12]. Furthermore, benzimidazole based compounds are important for their applications as anti-inflammatory, antioxidant, antiulcers, antihypertensives, antiviral, antifungals, antihistaminics and antiparasitic activities [13]. In addition, benzimidazoles can form stable complexes with different transition metals and their coordination chemistry continues receiving huge attention not only because of their interesting spectral, magnetic and structural properties [14], but also because metal complexes of benzimidazoles and its derivatives have shown therapeutic applications such as anticancer agents, antioxidant and enzyme inhibitors [15].

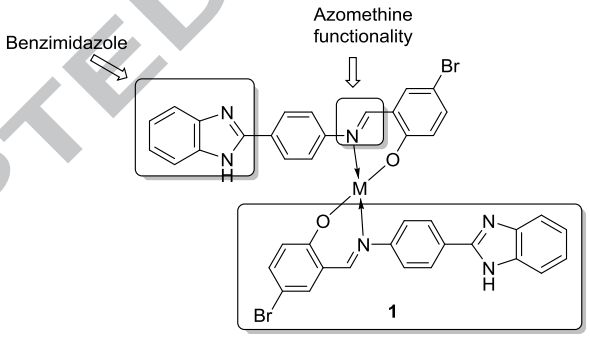

Figure 1. Structures of benzimidazole, azomethine (Schiff base) functionality, compound **1** and metallocomplexes [M= Zn(II), Pd(II), Ni(II), Cu(II)] proposed in this study.

A brief literature summary on the biological applications of (benz)imidazole Schiff base metal complexes has been recently reported [16]. Thus, it is stated that Ag(I), Zn(II), Sn(II) and Pd(II) complexes of these Schiff bases result in effective in vitro antimicrobial, antifungal and antibacterial activities [17]. Moreover, the azomethine functionality (-HC=N-) in the mentioned Schiff bases (Figure 1) seems to be responsible for the various biological activities of these compounds, for instance as

antibacterial [18,19], antifungal [20,21], anti-inflammatory [22] or anticancer/antitumor agents [23-25]. Additionally, it has been found that these biological activities are enhanced in their metal(II) complexes [26-30].

Keeping in mind the urgent need for new antibiotics and taking into account the suitability of benzimidazoles and Schiff bases as ligands in antibacterial metallodrugs, we present in this paper the preparation, biophysical and biochemical investigation of a new family of metal complexes of compound **1** (Figure 1). The effect on the biological activity of different metals such as Zn(II), Pd(II), Ni(II) and Cu(II), belonging to different groups and rows of the Periodic Table, was explored based on the bioactivity of related complexes. Thus, Zn(II), Pd(II), Ni(II) and Cu(II) derivatives have shown activity as antibacterial, antifungal and anticancer agents as mentioned before [6-8,15-17,26-30].

Additionally, the drug-DNA interaction was investigated by UV-vis spectroscopy titration and DNA thermal denaturation experiments as well as their antimicrobial activities against a number of Gram positive and Gram negative bacteria.

2. Material and Methods

2.1. General Information

All chemicals including solvents and reactant materials were purchased from Sigma Aldrich and were used without further purification. Salmon testes DNA [(st)DNA] was purchased from Sigma Aldrich (St Louis, MO, USA) and has an extinction coefficient ε_{260}= 6600 M^{-1} cm^{-1}. Infrared (IR) spectra were recorded on Perkin Elmer Spectrum One spectrometer in 4000-400 cm^{-1} region. ^{1}H and $^{13}C\{^{1}H\}$ NMR spectra were obtained on a Bruker Avance 400 and Bruker DPX 400, and were referenced to the residual ^{1}H and ^{13}C resonances of the solvent used. High resolution mass spectrometry analysis were carried out using a Premier Waters Maldi-quadrupole time-of-flight (Q-TOF) mass spectrometer

equipped with Z-spray electrospray ionization (ESI) and matrix assisted laser desorption ionization (MALDI) sources.

2.2. Synthesis

2.2.1. Preparation of 4-(1*H*-benzo[*d*]imidazole-2-yl)aniline (2)

In a two neck round bottom flask (250 mL) equipped with magnetic stirrer and reflux condenser, *o*-phenylenediamine and 4-aminobezoic acid were refluxed in polyphosphoric acid, in a 1:1 molar ratio. The reaction mixture was heated at 130 °C for 3 h. After the completion of reaction the thick liquid mixture was poured onto crushed ice, neutralized with 4N NaOH solution and precipitates were formed. The precipitate containing compound **2** was removed from the mother liquor by filtration and was used immediately for the preparation of compound **1**.

2.2.2. Preparation of (*E*)-2-((4-(1*H*-benzo[*d*]imidazol-2-yl)phenylimino) methyl)-4-bromophenol (1) [31]

Compound **1** was synthesized by condensing 4-(1*H*-benzo[*d*]imidazole-2-yl)benzenamine (**2**) (0.21 g, 1 mmol) and 5-bromosalicylaldehyde (0.2 g, 1 mmol) in dry ethanol under reflux for 6 hours. The resultant orange coloured precipitate was collected by filtration, washed with hot ethanol and recrystallized from THF. Yield: 81%. M.p.: 165 °C (Lit.: 161-165 °C [29]). IR (ν, cm^{-1}): 3451 (O-H), 3337 (N-H), 1619 (azomethine-C=N), 1558 (imidazole-C=N), 1436 (imidazole-C-N), 1262 (C-O). ^{1}H NMR (400 MHz, DMSO-d_6) δ (ppm): 6.96-8.29 (m, Ar), 8.86 (s, CH=N), 11.68 (bs, s, OH), 12.91 (s, NH). $^{13}C\{^{1}H\}$ NMR (400 MHz, DMSO-d_6) δ (ppm): 111.3-145.7 (Ar C), 162.0 (CH=N), 149.9 (imidazole CH=N). Anal. Calc. for $C_{20}H_{14}N_3OBr$: C, 61.24; H, 3.60; N, 10.71. Found: C, 61.27; H; 3.59, N; 10.69. HRMS (m/z) calculated for $C_{20}H_{15}N_3OBr$ [$M+H^+$] 392.0398, found 392.0394.

2.2.3. Preparation of the Zn(II) complex of compound 1 (3)

In a two neck round bottom flask (100 mL) equipped with magnetic stirrer and reflux condenser, a hot ethanolic solution of **1** (1 mmol) and a solution of $Zn(CH_3COO)_2 \bullet 2H_2O$ (0.5 mmol) were mixed in a 2:1 molar ratio and refluxed for 4 hours. A bright yellow precipitate was collected by filtration, washed with hot ethanol and recrystallized from THF. Yield: 73%. M.p.: >300 ^oC. IR (ν, cm^{-1}): 3367 (N-H), 1606 (azomethine-C=N), 1545 (imidazole-C=N), 1449 (imidazole-C-N), 1306 (C-O), 580 (M-O), 460 (M-N). ^1H NMR (400 MHz, DMSO-d_6) δ (ppm): 6.68-8.29 (m, Ar), 9.06 (s, CH=N), 13.06 (s, NH). $^{13}C\{^1H\}$ NMR (400 MHz, DMSO-d_6) δ (ppm): 112.34-145.64 (Ar C), 165.7 (CH=N), 150.91 (imidazole CH=N). Anal. Calc. for $C_{40}H_{26}N_6O_2ZnBr_2$: C, 56.66; H, 3.09; N, 9.91; Zn, 7.71. Found: C, 56.59; H, 3.03; N, 9.92; Zn, 7.72. HRMS (m/z) calculated for $C_{40}H_{26}N_6O_2ZnBr_2$ $[M+H^+]$ 847.9834, found 847.9817.

2.2.4. Preparation of the Pd(II) complex of compound 1 (4)

Compound **1** (1 mmol) was dissolved in hot ethanol in a two neck round bottom flask (100 mL) equipped with magnetic stirrer and reflux condenser. Then, a solution of $Pd(CH_3COO)_2$ (0.5 mmol) was added dropwise and the mixture refluxed for 3 hours. A dark brown precipitate was collected by filtration, washed with hot ethanol and recrystallized from THF. Yield: 65%. M.p.: >300 °C. IR (ν, cm^{-1}): 3356 (N-H), 1588 (azomethine-C=N), 1559 (imidazole-C=N), 1440 (imidazole-C-N), 1314 (C-O), 567 (M-O), 442 (M-N). ^1H NMR (400 MHz, DMSO-d_6) δ (ppm): 6.97-8.29 (m, Ar), 9.046 (s, CH=N), 12.97 (s, NH). $^{13}C\{^1H\}$ NMR (400 MHz, DMSO-d_6) δ (ppm): 114.2-133.2 (Ar C), 164.1 (azomethine CH=N), 150.0 (imidazole CH=N). Anal. Calc. for $C_{40}H_{26}N_6O_2PdBr_2$: C, 54.05; H, 2.95; N, 9.45; Pd, 11.97. Found: C, 54.16; H, 3.18; N, 9.51; Pd, 11.99. HRMS (m/z) calculated for $C_{40}H_{27}N_6O_2PdBr_2$ $[M+H^+]$ 886.9597, found 886.9602.

2.2.5. Preparation of the Ni(II) complex of compound 1 (5)

In a two neck round bottom flask (100 mL) equipped with magnetic stirrer and reflux condenser, ethanolic solutions of compound **1** (1 mmol) and $Ni(CH_3COO)_2 \bullet 4H_2O$ (0.5 mmol) were mixed in 2:1 molar ratio and refluxed for 3 hours. An orange precipitate was collected by filtration, washed with

hot ethanol and crystallized from THF. Yield: 60%. M.p.: 285 °C. IR (ν, cm^{-1}): 3365 (N-H), 1597 (azomethine-C=N), 1531 (imidazole-C=N), 1445 (imidazole-C-N), 1286 (C-O), 553 (M-O), 436 (M-N). ^{1}H NMR (400 MHz, DMSO-d_6) δ (ppm): 6.79-8.68 (m, Ar) 9.08(s, CH=N), 13.17(s, NH) $^{13}C\{^{1}H\}$ NMR (400 MHz, DMSO-d_6) δ (ppm): 115.28-135.53 (Ar, C), 170.14 (CH=N), 151.06 (imidazole CH=N). Anal. Calc. For $C_{40}H_{26}N_6O_2NiBr_2$: C, 57.11; H, 3.12; N, 9.99; Ni, 6.98. Found: C, 57.47; H, 3.23; N, 10.33; Ni, 6.91. HRMS (m/z) calculated for $C_{40}H_{28}N_6O_2NiBr_2$ $[M+H^+]$ 843.1935, found 843.1912.

2.2.6. Preparation of the Cu(II) complex of compound 1 (6)

In a two neck round bottom flask (100 mL) equipped with magnetic stirrer and reflux condenser, ethanolic solutions of compound **1** (1 mmol) and $Cu(CH_3COO)_2 \bullet 2H_2O$ (0.5 mmol) were mixed and refluxed for 6 hours. A greenish yellow precipitate was collected by filtration washed with hot ethanol and crystallized from THF. Yield: 80%. M.p.: 223 °C. IR (ν, cm^{-1}): 3349 (N-H), 1595 (azomethine-C=N), 1515 (imidazole-C=N), 1442 (imidazole-C-N), 580 (M-O), 420 (M-N). Anal. Calc. for $C_{40}H_{26}N_6O_2CuBr_2$: C, 56.79; H, 3.10; N, 9.93; Cu, 7.51. Found (%): C, 56.65; H, 3.02; N, 9.91; Cu, 7.46. HRMS (m/z) calculated for $C_{40}H_{28}N_6O_2CuBr_2$ $[M+H^+]$ 844.9936, found 844.9901.

2.3. Biophysical experiments

2.3.1. DNA thermal denaturation

Thermal melting experiments were conducted with Perkin Elmer Lambda 35 UV-VIS spectrometer, (TempLAB software). Temperatures were monitored with a thermistor inserted into a 1 mL quartz cuvette containing the same volume of water as in the sample cells. Absorbance changes at λ = 260 nm were monitored from a range of 30 to 90 °C in a gradient of 1 °C per min and measuring every 0.2 °C. A quartz cell with a 1 cm path length was filled with a 1 mL solution of (st)DNA or (st)DNA-ligand complex in DMSO:water mixture in 30:70 ratios by %volume, respectively. The (st)DNA

oligomer (100 μM) and the ligand solution (10 μM) were prepared in a phosphate buffer (0.01 M K_2HPO_4/KH_2PO_4), adjusted to pH 7 and syringe filtered, so that a ligand to DNA base ratio of 0.1 was obtained. Experiments were performed immediately after solutions were prepared to avoid decomposition. The difference in melting temperature (ΔT_m, °C) was calculated as factor of stability and the T_m was defined as the mid-point of transition temperature.

2.3.2. Absorption spectroscopic studies

The absorption spectroscopic and the thermal denaturation studies to assess the interaction between the ligands (compound **1** and its metal complexes) and DNA was carried out using Perkin Elmer Lambda 35 UV-vis spectrometer equipped with temperature control unit and temp lab software. For the titrations in the absorption spectroscopic study, stock solutions (500 μM) of Schiff base **1** and the four metal complexes were prepared in DMSO and for further dilutions (100 μM) deionized water was used. Salmon testes DNA [(st)DNA] was prepared in Tris-HCl buffer solution (0.6 M HCl) and 50 mM NaCl with pH = 7.33 and this buffered (st)DNA was filtered using syringe filtration method to make it protein free. DNA and ligand solution were incubated for 5 min before recording the absorption spectrum. A fixed amount (1000 μL) of the ligand (100 μM) was titrated with increasing quantity (10 to 80 μL) of DNA. The intrinsic binding constants or K_b (a measure of the strength of interaction between (st)DNA and the chromophores of the ligand) were calculated from the Benesi-Hildebrand equation [32].

$$\frac{A_0}{A-A_0} = \frac{\varepsilon_G}{\varepsilon_{H-G}-\varepsilon_G} + \frac{\varepsilon_G}{\varepsilon_{H-G}-\varepsilon_G} \times \frac{1}{K_b[DNA]}$$

where [DNA] represents the concentration of (st)DNA in base molarity; A_0 and A is the absorbance of the free drug and the drug in the presence of DNA, respectively; and ε_G and ε_{H-G} are the absorption coefficients of the drug and drug-DNA complex, respectively. Thus, the intrinsic binding constant K_b can be calculated from the intercept to slope ratio of $A_0/A-A_0$ *vs.* 1/[DNA] plots [33] .

2.4. X-Ray crystallographic analysis

A suitable crystal of ligand **1** was selected and data was collected on Bruker D8 Quest ECO diffractometer. The sample was mounted on a MiTeGen micromount and data was collected at 100(2) K using an Oxford Cryostream. Bruker APEX software was used to collect and reduce the data, determine the space group, solve and refine the structures [34]. Absorption corrections were applied using SADABS 2014 [35]. The structure was solved with the XT structure solution program [36] using Intrinsic Phasing and refined with the XL refinement package [37] using Least Squares minimization in Olex2 [38]. All non-hydrogen atoms were refined anisotropically. Hydrogen atoms were assigned to calculated positions using a riding model with appropriately fixed isotropic thermal parameters. Parameters and refinements for data collection are summarized in Table S1 (Supporting Information). CCDC 1566746 contains the supplementary crystallographic data for this paper. This data can be obtained free of charge from The Cambridge Crystallographic Data Centre via www.ccdc.cam.ac.uk/data_request/cif.

2.5. Biochemistry

2.5.1. Antibacterial disc diffusion assays

The antibacterial activity of the compounds was screened against *Escherichia coli*, *Enterobacter aerogenes* and *Micrococcus luteus*. The bacteria were cultured in nutrient broth under controlled conditions of temperature (37 °C) for 24 hours. From this cultured medium, 1% broth containing about 10^6 colony-forming units (CFU/mL) of bacterial strain was transferred to the nutrient agar medium at 45 °C and then poured into the sterile petri plates. When the medium was solidified, about 5 µL of the test compound (40 mg mL^{-1} in DMSO) was poured on sterile paper discs of 4 mm size and placed on nutrient agar plates respectively. In each plate the standard antibacterial drug kanamycin (1 mg mL^{-1}) served as a positive control and DMSO served as negative control. For each bacterial strain, the plates were prepared in triplicate. These plates were incubated for 24 hours at 37 °C with compounds **1**, **3-6** (200 µg mL^{-1}). The antibacterial activity was determined by measuring

the diameter of the zone of complete inhibition in mm when the concentration of the compounds was 200 μg mL^{-1}. Downstream calculations were done for the compounds which showed activity at this concentration (inhibition zone ≥10 mm) by making dilutions (200 μg mL^{-1}, 100 μg mL^{-1}, 50 μg mL^{-1}, 25 μg mL^{-1}, 12.5 μg mL^{-1}, 6.25 μg mL^{-1}, 3.12 μg mL^{-1}). Then, minimum inhibitory concentration (MIC) values for compounds **1**, **3-6**, defined as the lowest concentration of the compound that inhibits visible growth, and were calculated from the inhibition zone diameters via linear regression. All determinations were performed in triplicate.

3. Results and Discussion

3.1. Synthesis and characterization

The preparation of compound **1** had been reported in the literature by Cernatescu and Comanita [31] starting from precursor **2**; however, we have carried out the preparation of compound **1** following a slightly different method. First, precursor **2** was synthesized by the condensation of 2-aminoaniline and *p*-aminobenzoic acid in the presence of polyphosphoric acid at 130 °C (Scheme 1).

Scheme 1. Synthesis of **1** and its metal complexes

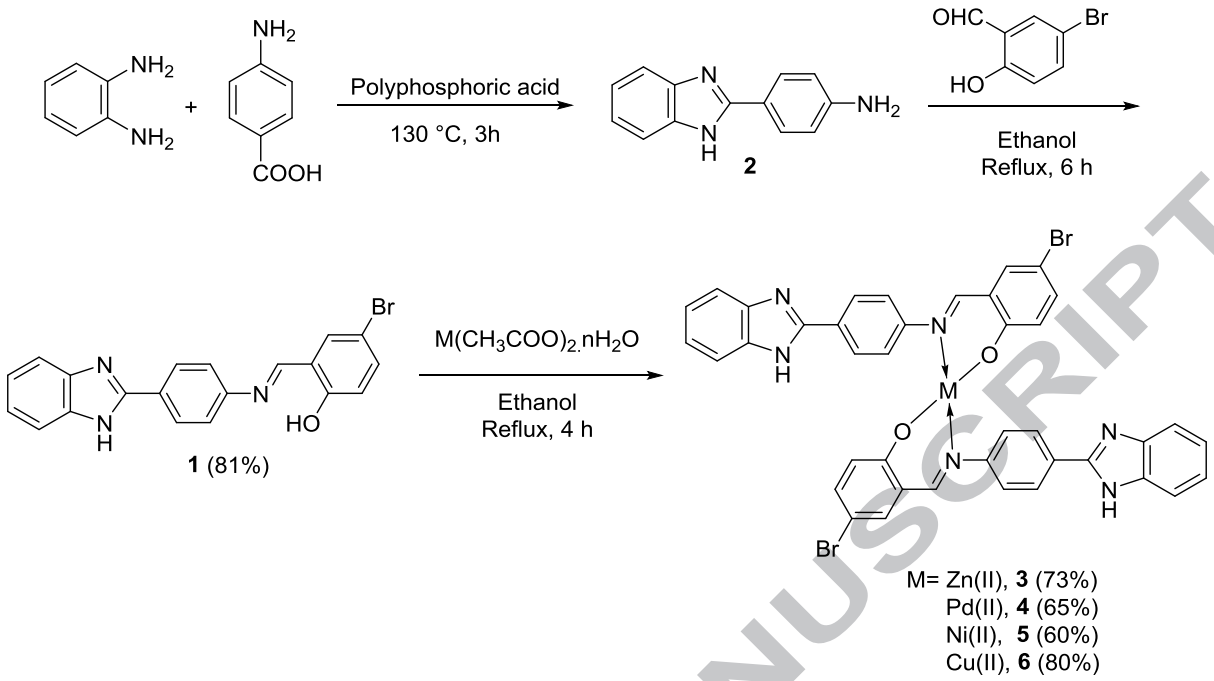

Then, without further purification, compound **2** was reacted with 4-bromo-2-hydroxybenzaldehyde in a reflux of ethanol forming compound **1** in an excellent yield (81%) without the need of acetic acid as a catalyst, as it had been previously reported [31], since traces of phosphoric acid from the previous step are present. The four new metal complexes **3**-**6** were successfully prepared by the reaction of **1** and the corresponding metal(II) acetate in refluxing ethanol (Scheme 1), in good to excellent yields (60-80%). All compounds prepared are stable under normal atmospheric conditions and soluble in organic solvents such as DMSO or DMF, whilst **4** and **6** are also partially soluble in ethanol. All were fully spectroscopically and analytically characterized.

The infrared spectrum of **1** showed a broad band at 3451 cm^{-1} assigned to the phenolic OH group and a low intensity band at 3377 cm^{-1} due to the N-H group of the imidazole ring. Strong bands at 1619, 1558 and 1436 cm^{-1} are assigned to the azomethine group (C=N), imidazole azomethine group (C=N) and imidazole C-N bond, respectively [39] . The IR spectra of the metal complexes showed a loss of the phenolic OH band and an increase in the ν(C-O) at 1286-1319 cm^{-1}, indicative of deprotonation and formation of a M-O bond. The bands associated with the imidazole fragment do not shift

indicating that this moiety does not coordinate to the metal centre. However, a shift of the C=N band associated with the azomethine group is observed, signifying its participation in bonding to the metal. The ν(M-O) and ν(M-N) bands in the 530-580 and 420-471 cm^{-1} region also confirm metal bonding.

Both ^{1}H and $^{13}C\{^{1}H\}$ NMR spectroscopy confirm binding of the ligand to the diamagnetic metal centres. The phenolic proton in **1** (δ_H = 11.68 ppm) is no longer present whilst there is a down-field shift of the azomethine proton (δ_H = 8.86 ppm in **1** to δ_H ~ 9.05 ppm in **3** and **4**), attributable to electron transfer from the Schiff base N atom to the metal ion [40]. Correspondingly, in the $^{13}C\{^{1}H\}$ NMR spectra the azomethine carbon shifts from δ_C = 162 ppm in **1** to δ_C = 165.7 ppm in **2** and **3**.

3.2. Single crystal X-Ray analysis

A single crystal of **1**·MeOH was obtained by the slow evaporation of a methanol solution under normal atmospheric conditions and the ordered arrangement of atoms in the molecule is shown in Figure 2a. Parameters and refinements for data collection are summarized in Table S1 (Supporting Information). This structure validates the spectroscopic data previously recorded. Metric parameters are normal and selected bond lengths and angles are presented in Table 1.

Table 1. Selected bond lengths (Å) and angles (°) for compound **1**

Bond length		Bond angle	
N(6)-C(7)	1.322(5)	O(24)-C(19)-C(20)	118.0(4)
C(7)-N(8)	1.351(5)	O(24)-C(19)-C(18)	122.6(3)
C(13)-N(16)	1.410(5)	C(17)-N(16)-C(13)	123.4(3)
N(16)-C(17)	1.284(5)	N(16)-C(17)-C(18)	120.1(4)
C(19)-O(24)	1.337(5)	C(7)-N(8)-C(9)	107.3(3)
O(24)-H(24)	0.8400		

It can be observed that all aromatic systems and the azomethine group are in the same plane. The most obvious feature is the strong intra and inter molecular hydrogen bonding formed by the hydroxyl groups in **1** and MeOH, e.g. O24-H24···N16 ($d_{O\cdots N}$ = 2.586(4) Å), O26-H26···N6 ($d_{O\cdots N}$ = 2.698(4) Å, see Figure 2b). Further intermolecular interactions are seen by the amide N8-H8···O26 ($d_{N\cdots O}$ = 2.733(4) Å).

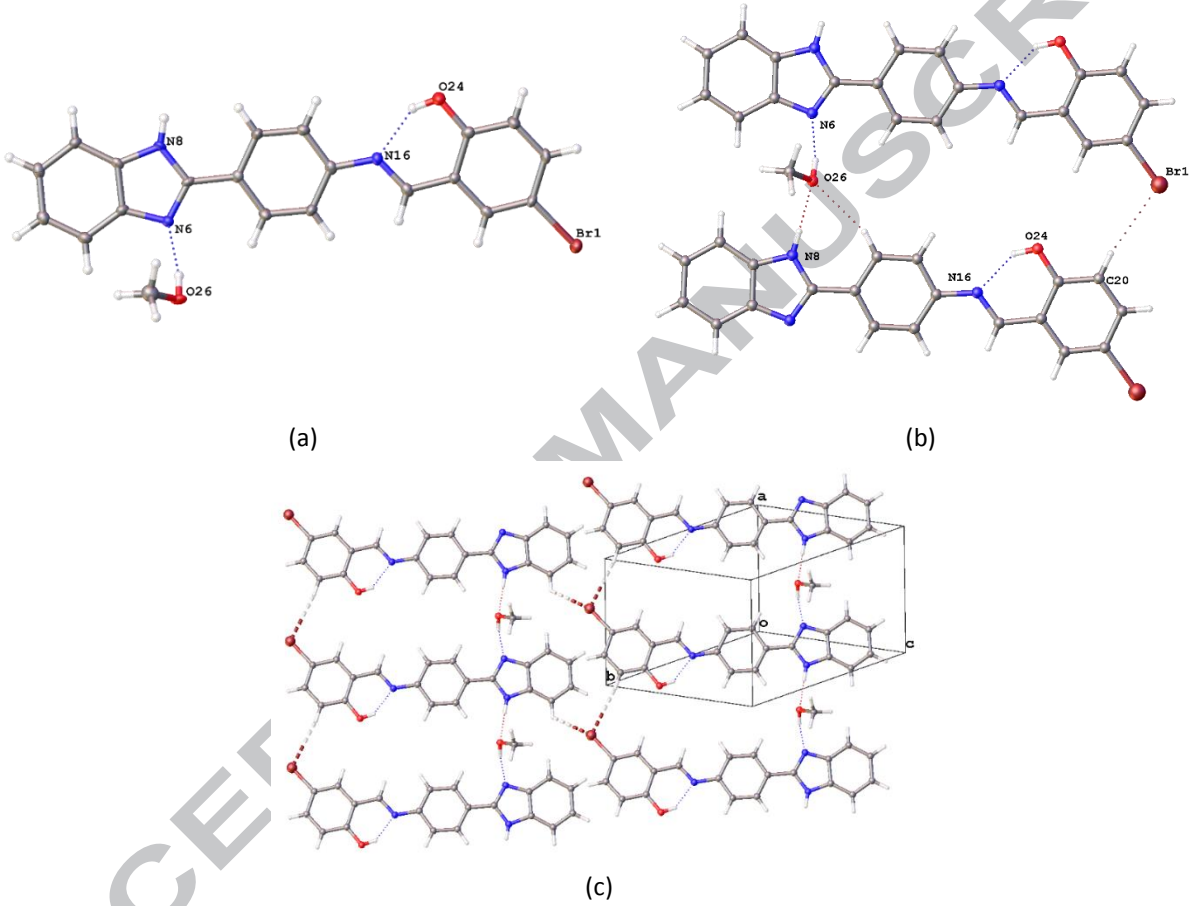

Figure 2. (a) Asymmetric unit of ligand **1** showing partial atom numbering and displacement ellipsoids (50% probability level). Dashed lines indicate H-bonding interactions; (b) intra/inter-molecular interactions (Br1···C20 = 3.998(4); Br1···C1 = 3.563(4) Å, O26···N6 = 2.698(4) Å, N8···O26 = 2.733(4) Å, O24···N16 = 2.586(4) Å); and (c) packing diagram of **1**·MeOH.

Moreover, intermolecular interactions such as π-π (between phenyl rings, 3.68 Å with a shift of 1.49 Å) and Br1···C20 and Br1···C1 [3.998(4) and 3.563(4) Å, see Figure 2b] are observed. Additionally, MeOH hydrogen bonding described above and other non-conventional hydrogen bonds [C15···O26, $d_{C\cdots O}$ = 3.452(5) Å] are combined to order the molecule in sheets as shown by the packing diagram in

Figure 2c. The ligand **1** adopted a P-1 space group symmetry with unit cell dimensions of a = 7.1625(5), b = 11.1249(9), c = 12.0359(9) Å and cell angles of α = 96.415(3), β = 96.576(3), γ = 105.598(3)°.

3.3. DNA binding studies: DNA thermal denaturation

Thermal denaturation experiments were employed, as detailed in our previous work [41], to assess the binding affinities of the compounds prepared to unspecific salmon testes DNA [(st)DNA]. It is well-known that when the temperature of a double stranded DNA solution increases, the double helix splits because of the dissociation of the hydrogen bonds between the base pairs. Accordingly, we can define the T_m melting temperature as that where half the bases dissociate from each other detected at 260 nm [42]. Depending on the magnitude of the interaction between a ligand and DNA, this T_m will shift (ΔT_m) indicating the strength of the interaction. Thus, T_m values of (st)DNA in the presence of compound **1** and its metal complexes **3-6** were obtained; the increments (ΔT_m) are collated in Table 2 and the plots are shown in Figure 3.

The ΔT_m value obtained after the addition of each ligand to (st)DNA indicates that, even though the values are small, **1** and its metal complexes bind to DNA. The free compound **1** as well as its Zn(II) and Ni(II) complexes present similar values of ΔT_m indicating a similar binding strength; in the case of the Pd(II) and Cu(II) complexes smaller values of ΔT_m are obtained indicating a weaker interaction. Therefore, the ΔT_m values meassured for the uncoordinated compound **1**, and the Zn(II) and Ni(II) complexes, **3** and **5** (3.3-3.2 ^oC) are the largest of this set, indicative of medium DNA binding. Considering that unspecific (st)DNA was used for these experiments, no specific information on the mode of binding to DNA can be extracted from the results; however, since the three ΔT_m values are very similar it could be deduced that the binding is driven by the ligand itself and the corresponding cations do not highly influence the interaction.

Table 2. Increments on (st)DNA thermal denaturation (ΔT_m, °C), binding constants (K_b, M^{-1}) and isobestic points (nm) found for compound **1** and metal complexes **3**-**6**.

	ΔT_m (°C)[a]	K_b (M^{-1})[b]	Isobestic points (nm)
1	3.3	1.47×10^5	338
3 [Zn(II)]	3.2	9.8×10^4	346
4 [Pd(II)]	2.3	6.0×10^3	-
5 [Ni(II)]	3.2	9.5×10^4	347
6 [Cu(II)]	2.8	3.1×10^4	353
Proflavin[42]	-	1.60×10^5	-

[a] The increment in DNA thermal melting (ΔT_m, °C) was measured in unspecific salmon testes DNA. Experiments were run in phosphate buffer (10 mM, pH 7). Thermal denaturation for natural (st)DNA = 68.5 °C. [b] Calculated from the $A_0/A\text{-}A_0$ *vs.* 1/[DNA] plots of the UV-vis DNA titrations results.

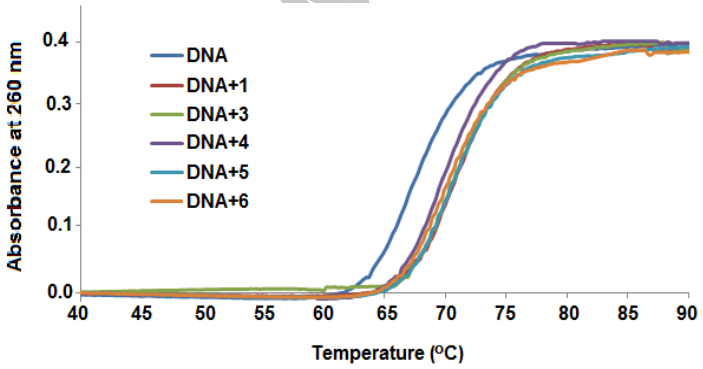

Figure 3. Thermal melting plots for (dark blue) (st)DNA (100 µM) in the presence of (red) compound **1**, (green) complex **3** [Zn(II)], (purple) complex **4** [Pd(II)], (light blue) complex **5** [Ni(II)] and (orange) complex **6** [Cu(II)].

3.4. DNA binding studies: UV-visible absorption spectroscopy

It is well known that UV-vis spectroscopy is a very useful technique to evaluate the binding ability of small molecules to DNA and it can provide information about the binding mode [43]. Thus, we have carried out UV-vis titration experiments with **1** and the metal complexes **3-6** by adding aliquots of (st)DNA. The interaction between any ligand and DNA is evident from the shifting either in

absorbance (hypochromic, hyperchromic) or in λ_{max} (hypsochromic, bathochromic). Intercalation of a ligand between the DNA base pairs results in the coupling of the π* orbital of the intercalator with the DNA base pairs, reducing the π→π* transition energy, and thus causing a red shift (bathochromism). Moreover, if the coupling π* orbital is partially filled with electrons it decreases the transition probabilities and a hypochromic shift in the absorbance can be observed [44]. Therefore, the presence of hypochromic and bathochromic shifts in the resulting UV-vis spectra of the titration of a ligand with (st)DNA indicates that such a ligand is an intercalator. The absorption spectra of the titration of **1**, **3**-**6** with (st)DNA are shown in Figure 4 and all the calculated K_b and isobestic points (nm) are presented in Table 2.

When the concentration of (st)DNA was increased a shift in absorbance as well as in λ_{max} was observed for most of the compounds. The absorption titration spectrum for DNA binding with **1** is shown in Figure 4a. Two isobestic points are observed, one at 338 and the other at 423 nm. The appearance of an isobestic point at 338 nm (Table 2) exemplifies that there are two chemical species, one being the free compound **1** and the other the DNA-**1** complex. Furthermore, a hypochromic shift in absorbance is observed along with a small bathochromic shift ($\Delta\lambda$ = 15 nm) to λ_{max} = 371 nm indicating the disappearance of the free compound **1** and the formation of the DNA-**1** complex. Hence, the λ_{max} bathochromic shift and hypochromic shift in absorbance suggest that compound **1** is an intercalator. The absorption spectra for the titration of **3**-**6** are shown in Figures 4b-e. Notably, the second isobestic point of **1** (at λ_{max} 423 nm) does not appear in the metal complexes. Among the complexes, Pd(II) complex **4** showed not only the smallest K_b value, but also neither a significant shift in absorbance or λ_{max} nor isobestic point indicating lack of interaction with DNA in agreement with the DNA thermal denaturation results.

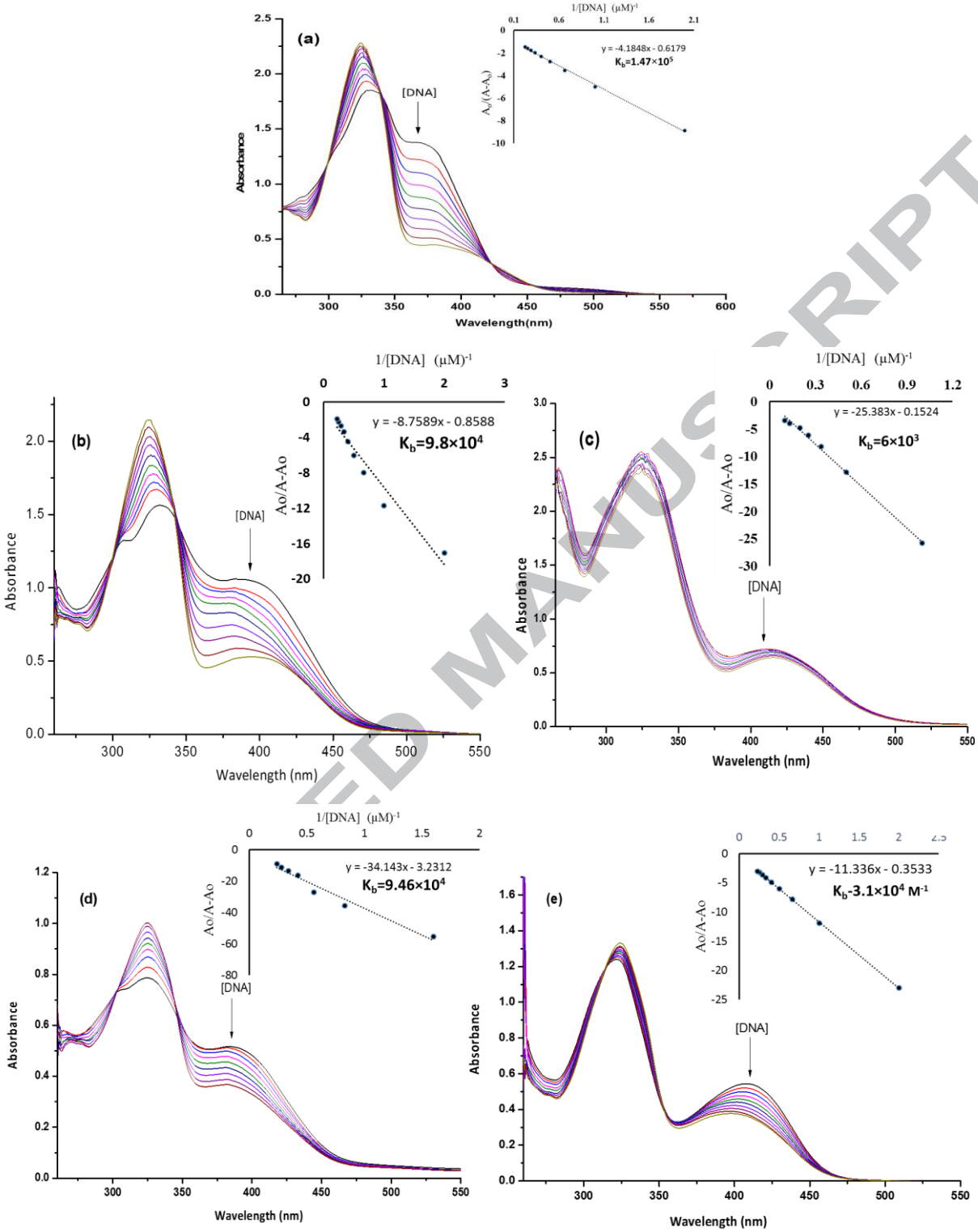

Figure 4. Changes in the UV-vis spectra of (a) compound **1** (b) complex Zn(II)-**1** (**3**) (c) complex Pd(II)-**1** (**4**) (d) complex Ni(II)-**1** (**5**) and (e) complex Cu(II)-**1** (**6**), having concentration 1×10^{-4} M, as a function of increasing quantities of (st)DNA (10-80 μM) in 50 mM Tris-HCl/NaCl buffer (pH= 7.35) at 25 °C. The arrows indicate the decrease in absorbance with increase in DNA concentration. Inset plots show $A_0/A\text{-}A_0$ *vs.* 1/[DNA] for the calculation of the corresponding intrinsic binding constant K_b.

The DNA binding constants for complexes **3, 5** and **6** (Table 2) indicate a stronger interaction than that of Pd(II) complex **4**, but weaker than for the free ligand **1**, which K_b compares well with that of the known intercalator proflavin [42]. As in the case of the uncoordinated ligand, isobestic points are observed for the DNA interaction with both complexes **3** and **5** (Table 2) indicating the existence of two species, the free metal complex (**3** or **5**) and DNA-complexes. The titration spectra of **3** shows a λ_{max} bathochromic shift and hypochromic shift in absorbance (Figure 3b) similar to **1** and, hence, DNA intercalation is expected. In the case of the Ni(II) complex **5**, the titration UV-vis spectra shows that a decrease in absorbance occurs with the addition of DNA aliquots (hypochromic effect); however, a hypsochromic effect is observed for the λ_{max}.

Summarizing, the strongest interaction with (st)DNA was exhibited by the ligand **1** in agreement with the DNA thermal denaturation experiments. The corresponding absorption spectra showed the appearance of an isobestic point indicating the formation of a DNA-**1** complex as well as a hypochromic effect along with a hypsochromic shift ($\Delta\lambda$ = 14 nm) to λ_{max} = 369 nm (Table 2). These results suggest that ligand **1** and complex **3** bind to DNA by intercalation mode while the absorption spectra of complexes **5** and **6** show binding to DNA by multiple modes but not intercalation [44].

The experimental results clearly indicate that compounds **1**, **3**, **5** and **6** interact with DNA since the distinct hypochromic effect suggests the formation of DNA-ligand complexes. The lack of DNA binding of the Pd(II) complex **4** could be attributed to the large atomic radius of the Pd(II) core (86 pm [45]) that hinders potential intercalation or minor groove binding.

Compound **1** and its Zn(II) complex (**3**) bind to DNA by intercalation with what could be justified on the one hand by the planarity of the Schiff base helped by the intramolecular hydrogen bond formed between the imino N atom and the phenolic OH (see Fig. 1), and on the other hand, the tetrahedral configuration of the Zn(II) complex, which allows for the intercalation of one of the ligand molecules

in between base pairs while the other stays perpendicular probably establishing extra interactions with the DNA strands. On the contrary, complexes **5** [Ni(II)] and **6** [Cu(II)], seem to interact with DNA by a different mode of binding. Typically, Ni(II) forms square planar complexes with Schiff base ligands (confirmed by the diamagnetic nature of **5**) and Cu(II) favours square planar geometries because of its d^9 electronic configuration [46]; hence, even though intercalation of one of the ligand moieties could still be allowed, no extra interaction of the second moiety with the DNA strands' phosphates would be expected. Moreover, under the oxidizing extracellular environment, copper exists as Cu(II), but in the reducing conditions inside the cell, it probably exists as Cu(I); that means that the metal core will have a larger radius that could interfere with the DNA binding. Additionally, Cu(II) complexes can induce reactive oxygen species (ROS) [47] damaging DNA.

3.5. Antibacterial activity

Compounds **1**-**6** were screened against three pathogenic bacterial strains: one Gram positive bacteria, *Micrococcus luteus* (ATCC 10240) and two Gram negative bacteria *Escherichia coli* (ATCC 15224) and *Enterobacter aerogenes* (ATTCC 13048) by applying the disc diffusion method [48,49]. Both Gram positive and negative bacteria were chosen to screen a broad antibiotic spectrum. The inhibition zone (measured in mm) and MIC (μg mL^{-1}) values obtained from triplicate measurements are shown in Table 3.

Even though less active than the positive control (kanamycin), in general, these compounds show antibacterial activity against both the Gram positive and Gram negative bacteria, with the exception of the Pd(II) and Cu(II) complexes (**4** and **6**) which were inactive against *E. coli* and *E. aerogenes*, respectively (Table 3). The metal complexes were more active against bacteria than the ligand **1**. Chelation of metal ions with Schiff base ligands enhances the lipophilicity of the ligand due to delocalization of π-electrons over the whole chelate system [50]. This enhanced lipophilicity

increases the penetration of the complexes through the lipid membranes into the cells facilitating the interaction with DNA.

Table 3. Antibacterial activities against *Micrococcus luteus*, *Escherichia coli* and *Enterobacter aerogenes* were measured in triplicate and expressed as inhibition zone (mm) and absolute MIC (μg mL^{-1}) values.

	Inhibition zone (mm)			**Absolute MIC (μg mL^{-1})**		
	M. luteus	***E. coli***	***E. aerogenes***	***M. luteus***	***E. coli***	***E. aerogenes***
1	6.0 ±0.2	17.0 ±1.2	9.0 ±0.9	166.7 ±4.5	60.2 ±2.6	111.1 ±5.0
3	11.0 ±0.8	18.9 ±1.5	13.6 ±0.8	90.9 ±3.9	52.9 ±3.1	73.9 ±3.7
4	9.0 ±0.5	-	12.0 ±1.0	111.1±5.0	-	81.7 ±1.9
5	16.8 ±1.1	18.8 ±1.6	13.0 ±1.2	58.9 ±2.2	53.0 ±4.4	76.9 ±4.6
6	14.9 ±1.0	11.8 ±0.9	-	67.1 ±3.1	84.4 ±4.8	-
K[a]	24.6 ±0.6	21.2 ±0.5	22.4 ±0.4	6.8 ±0.5	8.4 ±0.4	7.5 ±0.2

[a] Kanamycin.

The MIC values obtained for the antibacterial activity of the Ni(II) and Zn(II) complexes against *E. coli* and *E. aerogenes* follow a similar trend (Table 3); however the Cu(II) complex shows lower activity (for *E. Coli*) or no activity at all (*E. aerogenes*). Nevertheless, the results obtained for the antibacterial activities against *M. luteus* show that both the complexes **5** and **6** have very similar profile with better antibacterial activity than the Zn(II) complex. Hence, their biological activity seems to be dependent on the bacteria used.

Comparing the DNA binding and biological results obtained, we observe that even though the uncoordinated ligand (**1**) exhibits the best DNA binding, this is not reflected in its antibiotic activity maybe because this compound is not lipophilic enough to reach the nucleus of these microorganisms. The poor binding to DNA observed for complex **6** does not account for the relatively

good activity achieved against *M. luteus* and *E. Coli*. On the contrary, in the case of Zn(II) and Ni(II) complexes (**3** and **5**) a good correlation is observed between the DNA binding (K_b and ΔT_m values) and the MIC values obtained with *E. coli* and *E. aerogenes*.

Summarising, the best antibacterial results were obtained with the Ni(II) complex **5** in agreement with a good binding to DNA. The Zn(II) complex **3** shows a good antibacterial profile against the three organisms studied also in agreement to the DNA binding observed. Finally, Cu(II) complex **6** shows promising antibacterial activity against *M. luteus*, though not related to its poor DNA binding. Some studies have shown that the antibacterial properties of Cu(II) complexes could result from damaging the bacterial membrane inhibiting the expression of some extracellular proteins [51].

In order to have a preliminary assessment of the toxicity of these compounds, the brine shrimp lethality assay was performed at three different concentrations in triplicate along with DMSO as negative control and doxorubicin (LD_{50} value 7.3 μg mL^{-1}) as positive control (Table S2). The results showed that most of the compounds are, in principle, non-toxic with LD_{50} > 200 μg mL^{-1}. Only one compound (complex **6**) showed a LD_{50} value of 192.3 μg mL^{-1} which represents slight toxicity. These findings suggest that the synthesized compounds are non-toxic against shrimp.

4. Conclusions

An imidazole ring containing Schiff base ligand with 'O' and 'N' donor atoms and its metal complexes with different transition metals were successfully synthesized and fully characterized by different spectroscopic techniques.

DNA binding activity of all compounds was examined by thermal denaturation experiments and UV-vis absorption spectroscopy titrations. From the results obtained it can be concluded that the ligand

as well as most of its metal complexes have the ability to bind to (st)DNA by intercalation (compound **1** and its Zn(II) complex) or by other modes of binding (Ni(II) and Cu(II) complexes). Among all the compounds the free ligand is the stronger DNA binder while the Pd(II) complex is the weakest DNA binder.

Antimicrobial activity assays were also performed on both Gram positive and Gram negative bacteria and the results indicate that Ni(II), Zn(II) and Cu(II) complexes were good to moderate antibacterial agents with no toxicity in the brine shrimp assay with the exception of the Cu(II) complex which was slightly toxic.

Appendix A. Supplementary data

CCDC 1566746 contains the supplementary crystallographic data for compound **1**. These data can be obtained free of charge via http://www.ccdc.cam.ac.uk/conts/retrieving.html, or from the Cambridge Crystallographic Data Centre, 12 Union Road, Cambridge CB2 1EZ, UK; fax: (+44) 1223-336-033; or e-mail: deposit@ccdc.cam.ac.uk. Additionally, supplementary data containing ^{1}H and $^{13}C\{^{1}H\}$ NMR, IR and HRMS spectra of the compounds/complexes presented in this article is also available.

Acknowledgements

We thank the HEC Pakistan for funding this work.

References

[1] K. Lewis, *Nat. Rev. Drug Discov.* **2013**, *12*, 371-387.

[2] A. Bolhuis, J.R. Aldrich-Wright, *Bioorg. Chem.* **2014**, *55*, 51-59

[3] Y.S. Park, W.S. Shin, S.K. Kim, *J. Antimicrob. Chemother*. **2008**, *61*, 163-168.

[4] P. Nagababu, J.N.L. Latha, P. Pallavi, S. Harish, S. Satyanarayana, *Can. J. Microbiol*. **2006**, *52*, 1247-1254.

[5] T.A. Watt, C. Tong, A.P. Arnold, J.G. Collins. *Biochem. Mol. Biol. Int*. **1996**, *38*, 383-391.

[6] P. Fernandes, I. Sousa, L. Cunha-Silva, M. Ferreira, B. de Castro, E.F. Pereira, M.J. Feio, P. Gameiro, *J. Inorg. Biochem*. **2014**, *131*, 21-29.

[7] Among others: a) M.N. Patel, B.S. Bhatt, P.A. Dosi, *Appl. Biochem. Biotechnol*. **2012**, *166*, 1949-1968; b) M.N. Patel, B.S. Bhatt, P.A. Dosi, *Z. Anorg, Allg. Chem.* **2012**, *638*, 152-162; c) M.N. Patel, P.A. Dosi, B.S. Bhatt, *Med. Chem. Res*. **2012**, *21*, 2723-2733; d) S. Roy, K.D. Hagen, P.U. Maheswari, M. Lutz, A.L. Spek, J. Reedijk, G.P. van Wezel, *ChemMedChem* **2008**, *3*, 1427-1434; e) M. Cory, R.R. Tidwell, T.A. Fairley, *J. Med. Chem.* **1992**, *35*, 431-438; f) T.A. Shapiro, P.T. Englund, *Proc. Natl. Acad. Sci. USA* **1990**, *87*, 950-954.

[8] M. Montazerozohori, S. Zahedi, A. Naghiha, M.M. Zohour, *Mater. Sci. Eng. C*. **2014**, *35*, 195-204.

[9] H. Göker, S. Ölgen, R. Ertan, H. Akgün, S. Özbey, E. Kendi, G. Topçu, *J. Heterocycl. Chem.* **1995**, *32*, 1767–1773.

[10] U. Tawar, A.K. Jain, *J. Med. Chem.* **2003**, *46*, 3785-3792.

[11] Some recent examples: a) A.-L. Grillot, A. Le Tiran, D. Shannon, E. Krueger, Y. Liao, H. O'Dowd, Q. Tang, S. Ronkin, T. Wang, N. Waal, P. Li, D. Lauffer, E. Sizensky, J. Tanoury, E. Perola, T.H. Grossman, T. Doyle, B. Hanzelka, S. Jones, V. Dixit, N. Ewing, S. Liao, B. Boucher, M. Jacobs, Y. Bennani, P.S. Charifson, *J.Med. Chem*. **2014**, *57*, 8792-8816; b) P. Picconi, C. Hind, S. Jamshidi, K. Nahar, M. Clifford, M.E. Wand, J.M. Sutton, K.M. Rahman, *J. Med. Chem.* **2017**, *60*, 6045-6059; c) G.S. Bisacchi, J.I. Manchester, *ACS Infect. Dis.* **2015**, *1*, 4-1; d) H. Nimesh, S. Sur, D. Sinha, P. Yadav, P. Anand, P. Bajaj, J.S. Virdi, V. Tandon, *J. Med. Chem.* **2014**, *57*, 5238-5257.

[12] P. Prasad, I. Khan, P. Kondaiah, A.R. Chakravarty, *Chem. Eur. J.* **2013**, *19*, 17445–17455.

[13] For example, a) A. Sierra-Zenteno, C. A. Galan-Vidal, R. Tapia-Benavides, *Rev. Soc. Quím. Méx*. **2002**, *46*, 125–130; b) C. Rajarajeswari, R. Loganathan, M. Palaniandavar, E. Suresh, A. Riyasdeend, M.A. Akbarsha, *Dalton Trans.* **2013**, *42*, 8347-8363.

[14] Among others: a) I. Casanova, M. L. Durán, J. Viqueira, A. Sousa-Pedrares, F. Zani, J. A. Real, J. A. García-Vázquez, *Dalton Trans.* **2018**, *47*, 4325-4340. b) K. L. Haas, K. J. Franz, *Chem. Rev.* **2009**, *109*, 4921–4960.

[15] Among others: a) M. B. Farukh, A. Shamim , *Eur. J. Med. Chem*. **2005**, *40*, 1103-1110. b) H. Khalid, M. Hanif, M. A. Hashmi, T. Mahmood, K. Ayub, M. Monim-ul-Mehboob, *Mini-Rev. Med. Chem.*, **2013**, *13*, 1944-1956. c) M. Gocke, S. Utku, S. Gur, A. Ozkul, F. Gumus, *Eur. J. Med. Chem.* **2005**, *40*, 135-141. d) B. Roopashree, V. Gayathri, A. Gopi, K.S. Devaraju, *J. Coord. Chem.*, **2012**, *65*, 4023-4040. e) F. Saczewski, E. Dziemidowicz-Borys, P. J. Bednarski, R. Grünert, M. Gdaniec P. Tabin, *J. Inorg. Biochem.* **2006**, *100*, 1389-1398.

[16] G. Kumaravel, N. Raman, *Mater. Sci. Eng. C* **2017**, *70*, 184-194.

[17] Among others: a) M. Wang, L.F. Wang, Y.Z. Li, Q.X. Li, Z.D. Xu, D.Q. Qu, *Transit. Met. Chem.* **2001**, *26*, 307-323; b) M.A. Neelakantan, F. Rusalraj, J. Dharmaraja, S. Johnsonraja, T. Jeyakumar, M.S. Pillai, *Spectrochim. Acta, Part A* **2008**, *71*, 1599-1609; c) R.A. Hill, *Annu. Rep. Prog. Chem. Sect B* **2009**, *105*, 150-166; d) B. Forte, B. Malgesini, C. Piutti, F. Quartieri, A. Scolaro, G. Papeo, *Mar. Drugs* **2009**, *7*, 705-753; e) Z. Jin, *Nat. Prod. Rep.* **2011**, *28*, 1143-1191; f) G. Gao, R. Xiao, Y. Yuan, C.H. Zhou, J.S. You, R.G. Xie, *J. Chem. Res.* **2002**, 262-263; g) H.Y. Jiang, C.H. Zhouh, K. Luo, H. Chen, J.B. Lan, R.G. Xie, *J. Mol. Catal. A Chem.* **2006**, *260*, 288-294; h) A. Garoufis, S. K. Hadjikakou, N. Hadjiliadis, *Coord. Chem. Rev.* **2009**, *253*, 1384-1397.

[18] N. Raman, S. Sobha, A. Thamaraichelvan, *Spectrochim. Acta Mol. Biomol. Spectrosc*. **2011**, *78*, 888-898.

[19] P. Subbaraj, A. Ramu, N. Raman, J. Dharmaraja, *Spectrochim. Acta Mol. Biomol. Spectrosc*. **2014**, *117*, 65-71.

[20] N. Raman, S. Thalamuthu, J. Dhaveethuraja, M.A. Neelakandan, S. Banerjee, *J. Chil. Chem. Soc*. **2008**, *53*, 1439-1443.

[21] C.V.B. Martins, D.L. da Silva, A.T.M. Neres, T.F.F. Magalhaes, G.A. Watanabe, L.V. Modolo, A.A. Sabino, A. de Fátima, M.A. de Resende, *J. Antimicrob. Chemother*. **2009**, *63*, 337-339.

[22] A.M. Alafeefy, M.A. Bakht, M.A. Ganaie, M.N. Ansarie, N.N. El-Sayed, A.S. Awaad, *Bioorg. Med. Chem. Lett*. **2015**, *25*, 179-183.

[23] M.J. Chow, M.V. Babak, D.Y.Q. Wong, G. Pastorin, C. Gaiddon, W.H. Ang. *Mol. Pharmaceutics* **2016**, *13*, 2543-2554.

[24] Y. Lu, S. Wu, Y. Yue, S. He, J. Li, J. Tang, W. Wang, H.-B. Zhou, *ACS Med. Chem. Lett*. **2016**, *7*, 1185-1190.

[25] X. Zhou, L. Shao, Z. Jin, J.-B. Liu, H. Dai, J.-X. Fang, *Heteroat. Chem.* **2007**, *18*, 55-59.

[26] A. Lauria, R. Bonsignore, A. Terenzi, A. Spinello, F. Giannici, A. Longo, A.M. Almerico, G. Barone, *Dalton Trans.* **2014**, *43*, 6108-6119.

[27] M.B. Ferrari, S. Capacchi, G. Reffo, G. Pelosi, P. Tarasconi, R. Albertini, S. Pinelli, P. Lunghi, *J. Inorg. Biochem*. **2000**, *81*, 89-97.

[28] J. Charo, J.A. Lindencrona, L.M. Carlson, J. Hinkula, *J. Virol.* **2004**, *78*, 11321-11326.

[29] M. Wang, L.F. Wang, Y.Z. Li, Q.X. Li, Z.D. Xu, D.M. Qu, *Transition Met. Chem*. **2001**, *26*, 307-310.

[30] R.R. Hurtado, A.S. Harney, M.C. Heffern, R.J. Holbrook, R.A. Holmgren, T.J. Meade, *Mol. Pharm*. **2012**, *9*, 325-333.

[31] C. Cernatescu, E. Comanita, *Roumanian Biotechnological Lett.* **2006**, *11*, 2845-2850.

[32] H.A. Benesi, J.H. Hildebrand, *J. Am. Chem. Soc.* **1949**, *71*, 2703-2707.

[33] a) N. Na, D.Q. Zhao, H. Li, N. Jiang, J.Y. Wen, H.Y. Liu, *Molecules* **2016**, *21*, 54-68 ; b) I.E. Wachs, *Catal. Today* **1996**, *27*, 437-455; c) A. Pyle, J. Rehmann, R. Meshoyrer, C. Kumar, N. Turro, J.K. Barton, *J. Am. Chem. Soc*. **1989**, *111*, 3051-3058.

[34] Bruker APEX v2012.12-0, Bruker AXS Inc., Madison, Wisconsin, USA

[35] SADABS (2014) Bruker AXS Inc., Madison, Wisconsin, USA, Sheldrick, G. M. University of Göttingen, Germany

[36] G.M. Sheldrick, *Acta Cryst. A* **2015**, *71*, 3-8.

[37] G.M. Sheldrick, *Acta Cryst. A* **2008**, *64*, 112-122.

[38] O.V. Dolomanov, L.J. Bourhis, R.J. Gildea, J.A.K. Howard, H. Puschmann, *J. Appl. Cryst*. **2009**, *42*, 339-341.

[39] A.S. Orabi, A.M. Abbas, S.A. Salla, *Synth. React. Inorg. Met. Org. Chem*. **2013**, *43*, 63-75.

[40] S. Sathiyaraj, G. Ayyannan, C.J. Jayabalakrishnan, *Serb. Chem. Soc*. **2014**, *79*, 151-166.

[41] P.S. Nagle, F. Rodriguez, A. Kahvedžić, S. Quinn, I. Rozas, *J. Med. Chem*. **2009**, *52*, 7113-7121.

[42] A. Basu, G.S. Kumar, *J. Chem. Thermodynam.* **2015**, *87*, 1-7.

[43] C.Y. Zhou, J. Zhao, Y.B. Wu, C.X. Yin, Y. Pin, *J. Inorg. Biochem*. **2007**, *101*, 10-18.

[44] M. Bhowon, *Transition Met. Chem*. **2015**, *40*, 445-458.

[45] K. Ishida, T. Asao, *Bioconjugate Chem*. **2002**, *1587*, 155-163.

[46] A.F. Wells, Structural Inorganic Chemistry, 5th ed., Clarendon Press, Oxford, **1984**, pp. 1288.

[47] F.A. Cotton, G. Wilkinson, C.A. Murillo, M. Bochmann, Advanced Inorganic Chemistry, 6th edition, Wiley VCH.

[48] A. Sîrbu, O. Palamarciuc, M.V. Babak, J.M. Lim, K. Ohui, E.A. Enyedy, S. Shova, D. Darvasiová, P. Rapta, W.H. Ang, V.B. Arion, *Dalton Trans*. **2017**, *46*, 3833-3847.

[49] A. Felten, B. Grandry, P.H. Lagrange, I. Casin, *Int. J. Clin. Microbiol*. **2002**, *40*, 2766-2771.

[50] S. Arikan, V. Paetznick, J.H. Rex, *Antimicrob. Agents Chemother*. **2002**, *46*, 3084-3087.

[51] S. Rajalakshmi, A. Fathima, J.R. Rao, B.U. Nair, *RSC Adv.* **2014**, *4*, 32004-32012.